

Theory of Anderson pseudospin resonance with Higgs mode in superconductors

Naoto Tsuji¹ and Hideo Aoki¹

¹*Department of Physics, University of Tokyo, Hongo, Tokyo 113-0033, Japan*

(Dated: February 28, 2022)

A superconductor illuminated by an ac electric field with frequency Ω is theoretically found to generate a collective precession of Anderson's pseudospins, and hence a coherent amplitude oscillation of the order parameter, with a doubled frequency 2Ω through a nonlinear light-matter coupling. We provide a fundamental theory, based on the mean-field formalism, to show that the induced pseudospin precession resonates with the Higgs amplitude mode of the superconductor at $2\Omega = 2\Delta$ with 2Δ being the superconducting gap. The resonant precession is accompanied by a divergent enhancement of the third-harmonic generation (THG). By decomposing the THG susceptibility into the bare one and vertex correction, we find that the enhancement of the THG cannot be explained by individual quasiparticle excitations (pair breaking), so that the THG serves as a smoking gun for an identification of the collective Higgs mode. We further explore the effect of electron-electron scattering on the pseudospin resonance by applying the nonequilibrium dynamical mean-field theory to the attractive Hubbard model driven by ac electric fields. The result indicates that the pseudospin resonance is robust against electron correlations, although the resonance width is broadened due to electron scattering, which determines the lifetime of the Higgs mode.

PACS numbers: 74.25.N-, 74.40.Gh, 71.10.Fd

I. INTRODUCTION

Dynamical control of quantum many-body states of matter without destroying quantum coherence is becoming a central challenge in condensed matter physics. While recent developments in ultrafast laser experiments have enabled one to study relaxation dynamics of quantum systems after pulse excitation, an alternative direction we can pursue is to look at far-from-equilibrium quantum states that are realized *during photoirradiation*.

From this viewpoint, superconductivity is an intriguing ground to look for a novel optical control. A superconducting state can be described in terms of pseudospins introduced by Anderson in 1958.¹ Indeed, a collective precession of the pseudospins represents a Higgs amplitude mode¹⁻⁵, i.e., a coherent amplitude oscillation of the superconducting order parameter with a frequency 2Δ (the superconducting gap), which is a condensed matter analog of the Higgs boson in elementary particle physics,⁶⁻⁸ and the σ meson in nuclear physics.⁹ This naturally emerges as a massive mode along the radial direction in the Mexican-hat potential profile when a spontaneous symmetry breaking occurs in systems coupled to gauge fields^{6-8,10}. The Higgs mode in superconductors has been experimentally observed by Raman^{11,12} and THz pump-probe¹³ spectroscopies. A natural question then is whether one can manipulate the dynamics of the pseudospins like one does for real spins by applying a magnetic field. Usually, however, it has been supposed to be difficult to photo-control the pseudospins, since the pseudospins do not directly couple to electromagnetic fields (in the linear-response regime).

In this paper, we theoretically show that, if we go over to a *nonlinear* regime, an ac electric field with frequency Ω does indeed generate a collective precession of Anderson's pseudospins with frequency 2Ω through the nonlinear light-matter coupling, which results in a 2Ω amplitude oscillation of the superconducting order parameter. We further find that a *resonance* between the induced pseudospin precession and

the Higgs mode emerges when $2\Omega = 2\Delta$. This is remarkable, since this occurs *not* at $\Omega = 2\Delta$ but at Ω well below 2Δ (subgap regime), where quasiparticle excitations are suppressed. We may call the phenomenon “Anderson pseudospin resonance” (APR). APR may seem analogous to the nuclear magnetic resonance (NMR) or electron spin resonance (ESR), but APR is distinct in that the effect is essentially a *collective phenomenon as a resonance with the Higgs amplitude mode*. We show that APR should appear as a divergent enhancement of the third-order nonlinear optical response [third harmonic generation (THG)]. We further find that the enhancement of THG cannot be explained by quasiparticle excitations, which hence distinguishes the collective Higgs mode from individual pair breaking processes, both of which lie at the same energy scale. APR has been experimentally observed very recently by a THz laser experiment¹⁴.

II. PHENOMENOLOGICAL TIME-DEPENDENT GINZBURG-LANDAU THEORY

To understand how the order parameter and the Higgs amplitude mode dynamically respond to electromagnetic fields, it is instructive to first overview the time-dependent Ginzburg-Landau (GL) theory. This gives a simple macroscopic (and phenomenological) description of the superconducting order parameter as a low-energy effective field theory, although we have to mention that the time-dependent GL theory has a serious problem in describing the Higgs mode and its resonance in superconductors as we shall stress toward the end of this section, which makes us opt for a microscopic theory in later sections.

Let us consider the GL “Lagrangian density” as a functional

of the complex order parameter $\Psi(\mathbf{r}, t)$ in a general form of

$$\mathcal{L} = - \left[a|\Psi|^2 + \frac{b}{2}|\Psi|^4 + \frac{1}{2m^*} |(-i\nabla - e^*\mathbf{A})\Psi|^2 \right] + c|(i\partial_t - e^*\phi)\Psi|^2 + d\Psi^\dagger(i\partial_t - e^*\phi)\Psi \quad (1)$$

where a, b, c and d are coefficients, ϕ and \mathbf{A} are the scalar and vector potentials, and e^* and m^* are the effective electric charge and effective mass, respectively. The Lagrangian density (1) is invariant under the gauge transformation $\Psi(\mathbf{r}, t) \rightarrow e^{ie^*\chi(\mathbf{r}, t)}\Psi(\mathbf{r}, t)$, $\phi(\mathbf{r}, t) \rightarrow \phi(\mathbf{r}, t) - \partial_t\chi(\mathbf{r}, t)$, $\mathbf{A}(\mathbf{r}, t) \rightarrow \mathbf{A}(\mathbf{r}, t) + \nabla\chi(\mathbf{r}, t)$. At temperatures $T < T_c$, $a = a_0(T - T_c)$ becomes negative, and the global $U(1)$ symmetry [$\Psi(\mathbf{r}, t) \rightarrow e^{ie^*\chi}\Psi(\mathbf{r}, t)$ with a constant χ] is spontaneously broken. The other coefficients are taken to be positive. To describe the dynamics of the order parameter, we have included the kinetic terms, one with a coefficient c that represents the kinetic term of Klein-Gordon-type equations, and another with d that represents the kinetic term of Gross-Pitaevskii-type equations.

Now, we expand \mathcal{L} (1) around the ground state $\Psi_0 = \sqrt{-a/b}$ (the phase is chosen as such without loss of generality). There are two kinds of elementary excitations from the ground state: the variation along the radial direction and another along the circumferential direction on the complex plane of the order parameter. We write them as $\Psi(\mathbf{r}, t) = [\Psi_0 + H(\mathbf{r}, t)]e^{i\theta(\mathbf{r}, t)}$, where H and θ denote the Higgs and Nambu-Goldstone (NG) fields, respectively. The expansion gives us

$$\begin{aligned} \mathcal{L} = & c(\partial_t H)^2 + ce^{*2} \left(\phi + \frac{1}{e^*} \partial_t \theta \right)^2 (\Psi_0 + H)^2 \\ & - de^* \left(\phi + \frac{1}{e^*} \partial_t \theta \right) (\Psi_0 + H)^2 + 2aH^2 - \frac{1}{2m^*} (\nabla H)^2 \\ & - \frac{e^{*2}}{2m^*} \left(\mathbf{A} - \frac{1}{e^*} \nabla \theta \right)^2 (\Psi_0 + H)^2 + \dots \end{aligned} \quad (2)$$

in which we have dropped total-derivative terms as well as higher-order interactions.

The terms proportional to $\phi\partial_t\theta$ and $\mathbf{A} \cdot \nabla\theta$ in Eq. (2) indicate that the NG phase mode turns into a longitudinal component of the gauge field. As a result of the Anderson-Higgs mechanism,^{6-8,10} the NG mode is absorbed to the gauge field, and is pushed to very high energy scale of the plasma frequency ω_p . We can thus regard θ in Eq. (2) to be an unphysical degree of freedom, which one can eliminate by taking the unitary gauge,

$$\mathcal{L} = c(\partial_t H)^2 + (ce^{*2}\phi^2 - de^*\phi)(\Psi_0^2 + 2\Psi_0 H) + 2aH^2 - \frac{1}{2m^*} (\nabla H)^2 - \frac{e^{*2}\Psi_0^2}{2m^*} \mathbf{A}^2 + \frac{e^{*2}\Psi_0}{m^*} \mathbf{A}^2 H + \dots \quad (3)$$

One can see that the terms $ce^{*2}\phi^2$ and $\frac{e^{*2}\Psi_0^2}{2m^*} \mathbf{A}^2$ represent the mass of the gauge field generated via the Anderson-Higgs mechanism.

In the case of electrically neutral superfluids ($e^* = 0$), the Anderson-Higgs mechanism does not occur, so that the Higgs field mixes with the NG field via the term proportional to

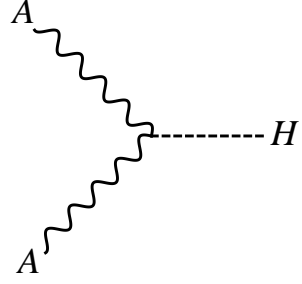


FIG. 1: The Feynman diagram for the interaction vertex that connects the Higgs field H (dashed line) and electromagnetic field \mathbf{A} (wavy lines).

$d(\partial_t\theta)H$ in Eq. (2), and the Higgs mode is no longer considered to be an isolated excitation. Furthermore, there are interactions between H and θ via the terms proportional to $c(\partial_t\theta)^2 H$ and $(\nabla\theta)^2 H$ in Eq. (2), which causes the relaxation of the Higgs into lower energy NG bosons, which makes the Higgs mode unstable. At this point, it has been often emphasized that the particle-hole symmetry is important in forcing $d \sim 0$ to suppress such a mixing between the Higgs and NG modes.^{4,5} In other words, the Higgs mode is to be protected by the particle-hole symmetry. However, this argument for the stability of the Higgs mode is not needed in the case of charged superconductors (although the particle-hole symmetry is a good symmetry near the Fermi surface in superconductors), since *the NG field decouples from the Higgs field [in Eq. (3)] due to the Anderson-Higgs mechanism* as stated above.

Equation (3) suggests that the interaction between the Higgs and gauge fields is given by ϕH , $\phi^2 H$ and $\mathbf{A}^2 H$. The linear coupling ϕH is suppressed in superconductors due to the inherent particle-hole symmetry ($d \sim 0$). The leading interaction is the second-order process $\phi^2 H$ and $\mathbf{A}^2 H$, the latter of which, e.g., is represented by a Feynman diagram shown in Fig. 1. The nonlinear Higgs-gauge coupling implies that H describes a scalar boson having no electric charge. These nonlinear couplings ($\phi^2 H$ and $\mathbf{A}^2 H$) have indeed been used in the discovery of the Higgs particle at the LHC experiment^{15,16} (where \mathbf{A} corresponds to the vector bosons W or Z).

From Eq. (3) (with $d = 0$), we can derive the equation of motion for the Higgs field,

$$\left(c\partial_t^2 - \frac{1}{2m^*} \nabla^2 \right) H = 2aH + e^{*2}\Psi_0 \left(c\phi^2 - \frac{1}{2m^*} \mathbf{A}^2 \right), \quad (4)$$

which is “relativistic” (with an emergent Lorentz symmetry),⁵ meaning that the first time-derivative is absent even though we started from the non-relativistic GL Lagrangian (1). Let us first look at the case of $\phi = \mathbf{A} = 0$. By putting $H(\mathbf{r}, t) \sim e^{iq \cdot \mathbf{r} - i\omega t}$, we obtain the dispersion relation for the Higgs mode,

$$\omega(\mathbf{q})^2 = -\frac{2a}{c} + \frac{q^2}{2m^*c} = \omega_H^2 + \frac{q^2}{2m^*c}, \quad (5)$$

where the mode is a gapped (massive) excitation with a char-

acteristic frequency (mass)

$$\omega_H = \sqrt{-\frac{2a}{c}}. \quad (6)$$

From this, one can see that $\omega_H \propto (T_c - T)^{1/2} \propto \Delta$. In fact, the microscopic calculation^{1,3} shows that $\omega_H = 2\Delta$, which exactly coincides with the lowest energy necessary to create a pair of Bogoliubov quasiparticles. Using the microscopic result¹⁷ of $b(\Psi_0/\Delta)^2 = 3/(4\epsilon_F)$ (with ϵ_F the Fermi energy), we have $c = -2a/(2\Delta)^2 = 2b\Psi_0^2/(2\Delta)^2 = 3/(8\epsilon_F)$. With this and $m^* = 2m$, we reproduce the well-known relation,³

$$\omega(\mathbf{q})^2 = (2\Delta)^2 + \frac{1}{3}v_F^2 q^2, \quad (7)$$

where $v_F = \sqrt{2\epsilon_F/m}$ is the Fermi velocity. From Eq. (2), it is obvious that the dispersion for the NG mode (or Bogoliubov mode) shares the same form $\omega(\mathbf{q})^2 = q^2/(2m^*c) = v_F^2 q^2/3$ with the Higgs mode besides the mass term. This agrees with the previously known result.¹⁸

Next, we turn to a situation where the system is driven by a continuous and homogeneous ac electric field $\mathbf{A}(t) = \mathbf{A}e^{-i\Omega t}$. The problem becomes equivalent to a forced oscillation of a harmonic oscillator, and the solution for Eq. (4) is given by

$$H(t) = \frac{1}{(2\Omega)^2 - \omega_H^2} \frac{e^{*2}\Psi_0 A^2}{2m^*c} e^{-2i\Omega t}. \quad (8)$$

This captures the fundamental aspect of the resonance phenomenon discussed in the paper. Due to the nonlinear coupling to the electric field, the elementary frequency of the oscillation of the Higgs field is 2Ω (rather than Ω). When 2Ω matches with the eigenfrequency of the Higgs field ω_H , the resonance occurs and the oscillation amplitude diverges as $(2\Omega - \omega_H)^{-1}$. From a microscopic point of view, this phenomenon can be understood as a resonant precession of Anderson pseudospins as we shall discuss in Sec. III.

The current $\mathbf{j} = \partial\mathcal{L}/\partial\mathbf{A}$ is expressed as

$$\mathbf{j} = -\frac{ie^*}{2m^*}[\Psi^\dagger \nabla \Psi - (\nabla \Psi^\dagger)\Psi] - \frac{e^{*2}}{m^*} \mathbf{A} \Psi^\dagger \Psi.$$

Expanding Ψ around Ψ_0 , we obtain the leading nonlinear current response against \mathbf{A} ,

$$\mathbf{j}_{\text{NL}}(t) = -\frac{2e^{*2}\Psi_0}{m^*} \mathbf{A}(t)H(t).$$

This takes the form of a London equation, where the current is proportional to $\mathbf{A}(t)$. Remarkably, the nonlinear current is also *proportional to the Higgs field* $H(t)$, so that the current can, and does indeed, sensitively reflect the temporal change of the Higgs field. Since $\mathbf{A}(t)$ oscillates with frequency Ω , while $H(t)$ oscillates with 2Ω , the current $[\propto \mathbf{A}(t)H(t)]$ ends up with oscillating with frequency 3Ω . This implies that a *giant third harmonic generation* (THG) is induced near the resonance ($2\Omega \sim \omega_H$) with the Higgs mode.

So far, we have discussed the Higgs mode and its resonance with electromagnetic waves based on the time-dependent GL

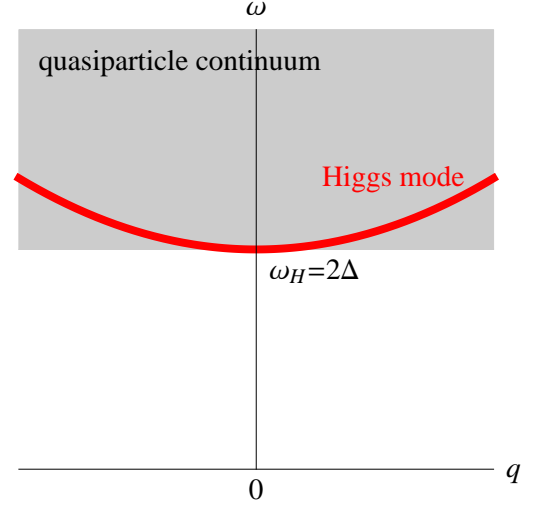


FIG. 2: (Color online) Schematic excitation spectrum of *s*-wave superconductors. The red curve is the collective Higgs mode, while the shaded region represents the quasiparticle excitation continuum.

theory (1). Apart from the fact that the characteristic frequency ω_H of the Higgs mode cannot be determined within GL theory, the problem of GL theory is that it does not take account of relaxations of the Higgs mode into quasiparticles. As shown in Fig. 2, the Higgs mode is degenerate with the lower bound of the quasiparticle excitation continuum ($\omega_H = 2\Delta$). The coincidence of the two energies is known as the Nambu relation.^{19,20} Since the Higgs mode lies at the same energy scale as the quasiparticle excitations, it can easily decay into individual quasiparticles. Furthermore, at low temperatures the relaxation time of quasiparticles becomes much longer than the time scale of the order-parameter variation in clean superconductors. As a result, one cannot neglect quasiparticle excitations, and the dynamics of the order parameter is necessarily entangled with those of quasiparticles. The low-energy effective theory of the Higgs mode may not be expressed only in terms of Ψ , but may involve fermionic degrees of freedom. The crucial questions that arise are (i) whether the Higgs resonance discussed here would survive or not after we take account of the relaxation to quasiparticles (pair-breaking process), and (ii) if it would survive, then how one can distinguish the collective Higgs mode from individual quasiparticle excitations, both of which are energetically degenerate. These motivate us to move on to the underlying microscopic theory in the subsequent sections.

III. MICROSCOPIC THEORY FOR ANDERSON PSEUDOSPIN RESONANCE

Having identified the necessity of going beyond GL theory, we start from the pairing Hamiltonian for an *s*-wave super-

conductor coupled to a dynamical electric field,

$$H_{\text{pair}} = \sum_{k,\sigma} \epsilon_{k-eA(t)} c_{k\sigma}^\dagger c_{k\sigma} - U \sum_{k,p} c_{k\uparrow}^\dagger c_{-k\downarrow}^\dagger c_{-p\downarrow} c_{p\uparrow}, \quad (9)$$

where ϵ_k is the band dispersion measured from Fermi energy ϵ_F , e the elementary charge, $A(t) = A \sin \Omega t$ the vector potential for the ac electric field $E(t)$ introduced by Peierls substitution (in the temporal gauge), $c_{k\sigma}^\dagger$ the creation operator for electrons, and $-U (< 0)$ is the attractive pairing interaction. We consider a superconducting thin film, into which the electric field can penetrate. For H_{pair} (9), the BCS mean-field description becomes exact. We define the superconducting gap function,

$$\Delta = \Delta' + i\Delta'' = U \sum_k \langle c_{k\uparrow}^\dagger c_{-k\downarrow}^\dagger \rangle, \quad (10)$$

that serves as the order parameter in the BCS theory. We can replace the momentum sum with an integral $D(\epsilon_F) \int_{-\omega_D}^{\omega_D} d\epsilon$ with $D(\epsilon_F)$ the density of states at the Fermi energy and ω_D the energy cut off (e.g., the Debye frequency of the bosonic pairing glue such as phonons). The interaction strength is characterized by a dimensionless $\lambda = UD(\epsilon_F)$. In the following we set $\hbar = 1$, and use ω_D as the unit of energy.

Anderson's pseudospin¹ is defined by

$$\sigma_k = \frac{1}{2} \Psi_k^\dagger \cdot \tau \cdot \Psi_k, \quad (11)$$

where $\Psi_k = (c_{k\uparrow}, c_{-k\downarrow}^\dagger)^t$ is the Nambu spinor, and $\tau = (\tau^x, \tau^y, \tau^z)$ are the Pauli matrices. The pseudospin satisfies the usual commutation relations for angular momentum, $[\sigma_k^j, \sigma_k^k] = i\epsilon_{jkl}\sigma_k^l$. With this, the pairing Hamiltonian (9) is recast in a form,

$$H_{\text{pair}} = 2 \sum_k \mathbf{b}_k \cdot \sigma_k, \quad (12)$$

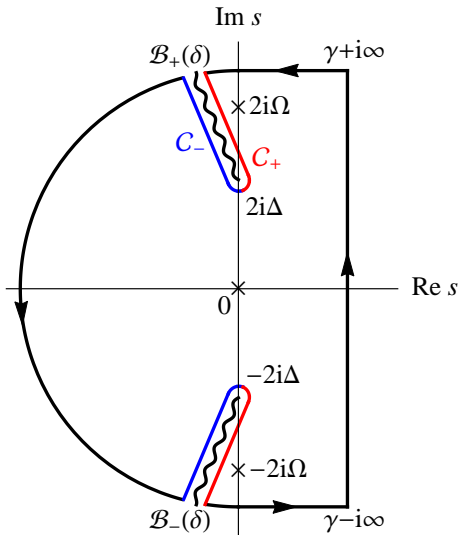


FIG. 3: (Color online) The integral contour (solid closed curve) that we take on the complex plane to evaluate the integral (22). Crosses and wavy lines represent poles and branch cuts, respectively.

which can be regarded as a spin system in an effective magnetic field,

$$\mathbf{b}_k = \left(-\Delta', -\Delta'', \frac{\epsilon_{k-eA(t)} + \epsilon_{k+eA(t)}}{2} \right). \quad (13)$$

The z component of \mathbf{b}_k represents the light-matter coupling involving contributions from both the particle and hole sectors. Since \mathbf{b}_k is a function even in $A(t)$ if the system is parity symmetric ($\epsilon_{-k} = \epsilon_k$), we can readily recognize that the linear coupling vanishes, so that the leading effect of the electric field starts from $O(A(t)^2)$. The self-consistency condition (10) reads

$$\Delta = U \sum_k (\sigma_k^x + i\sigma_k^y) \quad (14)$$

in the pseudospin notation. While the dynamics cannot be described by the conventional GL equation, which would be valid only when the time scale of the order-parameter motion is much longer than that of quasiparticle relaxations, in the present formalism the time evolution is determined by a Bloch equation for the pseudospins,^{2,21,22}

$$\partial_t \sigma_k = i[H_{\text{pair}}, \sigma_k] = 2\mathbf{b}_k \times \sigma_k. \quad (15)$$

Anderson pseudospins have been recently used to analyze the dynamics of charge fluctuations in a time-resolved Raman experiment for high- T_c cuprates.^{23,24}

We can analytically solve Eq. (15) up to the leading (second) order in $A(t)$. This is achieved by linearizing Eq. (15) with the time-independent and time-dependent parts separated as $\sigma_k(t) = \sigma_k(0) + \delta\sigma_k(t)$ and $\Delta(t) = \Delta + \delta\Delta(t)$. We assume that the initial state is superconducting at zero temperature. The initial Δ may be taken to be real positive without loss of generality. Thus the initial condition reads $\sigma_k^x(0) = \Delta/\omega_k$ and $\sigma_k^z(0) = -\epsilon_k/\omega_k$ with $\omega_k = 2(\epsilon_k^2 + \Delta^2)^{1/2}$. The linearized equations of motion are

$$\partial_t \delta\sigma_k^x(t) = -2\epsilon_k \delta\sigma_k^y(t), \quad (16)$$

$$\begin{aligned} \partial_t \delta\sigma_k^y(t) &= 2\epsilon_k \delta\sigma_k^x(t) + 2\Delta \delta\sigma_k^z(t) \\ &+ \frac{1}{\omega_k} \left[e^2 \Delta \sum_{ij} \partial_{k_i} \partial_{k_j} \epsilon_k A_i(t) A_j(t) - 2\epsilon_k \delta\Delta(t) \right], \end{aligned} \quad (17)$$

$$\partial_t \delta\sigma_k^z(t) = -2\Delta \delta\sigma_k^y(t). \quad (18)$$

Note that $\partial_t(\Delta\delta\sigma_k^x - \epsilon_k\delta\sigma_k^z) = 0$. From this, along with the initial condition $\delta\sigma_k(0) = 0$, it turns out that the relation $\Delta\delta\sigma_k^x = \epsilon_k\delta\sigma_k^z$ holds all the time, which helps us to reduce the number of the equations.

We solve the equations by a Laplace transformation, $\mathcal{L}[\delta\Delta(t)](s) =: \delta\Delta(s)$, etc. Let us call the direction of the electric field x . Then we have $\sum_{ij} \partial_{k_i} \partial_{k_j} \epsilon_k A_i(t) A_j(t) = \partial_{k_x}^2 \epsilon_k |A(t)|^2$. When the crystallographic directions are equivalent, we have $\partial_{k_x}^2 \epsilon_k \rightarrow d^{-1} \nabla_k^2 \epsilon_k$ with d the spatial dimension. If the band dispersion is isotropic with $\epsilon_k = \epsilon(|\mathbf{k}|)$, we expand ϵ_k around the Fermi wave number k_F as $\epsilon_k = \sum_{n=1}^{\infty} c_n (|\mathbf{k}| - k_F)^n$. With this, we can define a series expansion,

$$d^{-1} \nabla_k^2 \epsilon_k = \alpha_0 + \alpha_1 \epsilon_k + \alpha_2 \epsilon_k^2 + \cdots, \quad (19)$$

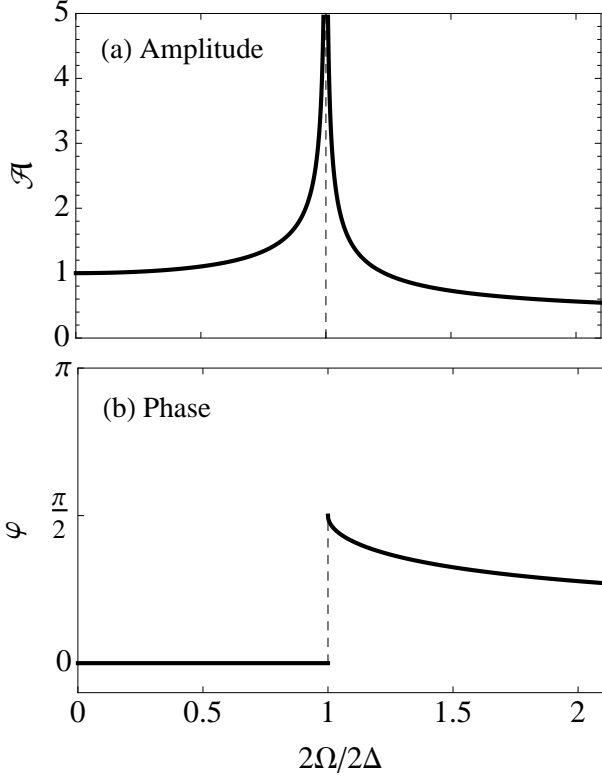


FIG. 4: (a) The amplitude \mathcal{A} and (b) phase shift φ of the 2Ω oscillation of the superconducting order parameter $\delta\Delta(t)$ [Eq. (23)] against $2\Omega/2\Delta$.

where $\alpha_0 = 2c_2d^{-1} + c_1(1 - d^{-1})k_F^{-1}$, $\alpha_1 = c_1^{-1}[6c_3d^{-1} + (1 - d^{-1})(2c_2k_F^{-1} - c_1k_F^{-2})]$, etc., with each coefficient $\alpha_n \sim O(\epsilon_F^{1-n})$. Since the α_0 term just gives a trivial phase $\exp(i\alpha_0 e^2 \int_0^t dt' A(t')^2)$ to $\Delta(t)$, which can be gauged out, the α_1 term provides the leading contribution around the Fermi surface (with $\omega_D \ll \epsilon_F$). For anisotropic band structures, the same expansion is still sometimes possible. For instance, the d -dimensional cubic lattice (with cosine bands $\epsilon_k = -2 \sum_i \cos k_i - \epsilon_F$) has $d^{-1} \nabla_k^2 \epsilon_k = \alpha_0 + \alpha_1 \epsilon_k$ with $\alpha_0 = -\epsilon_F d^{-1}$ and $\alpha_1 = -d^{-1}$.

Thus, in most cases of our interest, we arrive at

$$\frac{\delta\Delta(s)}{\alpha_1 e^2 A^2 \Delta} = \frac{\Omega^2}{s(s^2 + 4\Omega^2)} \left[1 - \frac{1}{\lambda(s^2 + 4\Delta^2)F(s)} \right], \quad (20)$$

where $A = |A|$ and

$$F(s) = \int_{-\infty}^{\infty} d\epsilon \frac{1}{2\sqrt{\epsilon^2 + \Delta^2}(s^2 + 4\epsilon^2 + 4\Delta^2)} = \frac{1}{s\sqrt{s^2 + 4\Delta^2}} \sinh^{-1} \left(\frac{s}{2\Delta} \right). \quad (21)$$

In the above, we have replaced the range of integration from $\int_{-\omega_D}^{\omega_D}$ to $\int_{-\infty}^{\infty}$, which is allowed in the BCS regime ($\omega_D \gg \Delta$). $F(s)$ can be analytically continued on the complex plane, where branch cuts $\mathcal{B}_{\pm}(\delta) = \{\pm 2i\Delta \pm ire^{\pm i\delta} | r \in [0, \infty)\}$ with δ small but nonzero are introduced (Fig. 3).

To obtain $\delta\Delta(t)$ with an inverse Laplace transformation, we need to evaluate a Bromwich integral,

$$I(t) = \frac{1}{2\pi i} \int_{\gamma-i\infty}^{\gamma+i\infty} ds e^{st} \frac{\Omega^2}{s(s^2 + 4\Omega^2)(s^2 + 4\Delta^2)F(s)}, \quad (22)$$

where $\gamma \in \mathbb{R}$ is taken to be larger than any of the real parts of the poles in the integrand. There are three first-order poles at $s = 0, \pm 2i\Omega$ and two branching points at $s = \pm 2i\Delta$ (Fig. 3) in the integrand, where $s = \pm 2i\Delta$ corresponds to the Higgs amplitude mode, while $s = \pm 2i\Omega$ to the forced precession of the Anderson pseudospins driven by the electric field. As one changes Ω , the poles merge with the branching points at $2\Omega = 2\Delta$, which causes a *resonance* between the forced pseudospin precession and the Higgs mode.

To make it more explicit, we evaluate the integral (22) by taking the contour as depicted in Fig. 3, which surrounds the three poles but avoids the branch cuts. This kind of contour is often used to calculate similar integrals (see, e.g., Ref.²). We take $\delta > 0$ so that the contours along the branch cuts $\mathcal{B}_{\pm}(\delta)$ do not touch the poles $s = \pm 2i\Omega$ when $\Omega > \Delta$. Since the contributions from infinity vanish, we are left with the residues of the poles and the line integrals (\mathcal{C}_{\pm} in Fig. 3 and their Hermitian conjugates) along the branch cuts. The asymptotic behavior of the integrals \mathcal{C}_{\pm} for $t \rightarrow \infty$ is evaluated by the saddle-point method. Finally we end up with long-time asymptotic forms of the order parameter,

$$\frac{\delta\Delta(t)}{\alpha_1 e^2 A^2 \Delta} \sim \frac{1}{4\lambda} \left[\frac{2}{\pi^{3/2}} \frac{\Omega^2}{\Omega^2 - \Delta^2} \frac{1}{\sqrt{\Delta t}} \cos \left(2\Delta t + \frac{\pi}{4} \right) - 1 \right] + \frac{1 - \cos 2\Omega t}{4} + \frac{1}{4\lambda} \times \begin{cases} \frac{\Omega}{\sqrt{\Delta^2 - \Omega^2}} \frac{\cos 2\Omega t}{\sin^{-1} \left(\frac{\Omega}{\Delta} \right)} & \Omega < \Delta \\ \frac{\Omega}{\sqrt{\Omega^2 - \Delta^2}} \frac{\cos(2\Omega t - \varphi)}{\sqrt{[\cosh^{-1} \left(\frac{\Omega}{\Delta} \right)]^2 + \left(\frac{\pi}{2} \right)^2}} & \Omega > \Delta \end{cases}, \quad (23)$$

where φ is the phase shift given by

$$\varphi = \tan^{-1} \left(\frac{\pi/2}{\cosh^{-1} \left(\frac{\Omega}{\Delta} \right)} \right). \quad (24)$$

The first term in Eq. (23) can be interpreted as the Higgs

amplitude mode induced by an effective change of the interaction parameter due to the ac field, $U \rightarrow U_{\text{eff}} = (1 - \frac{1}{2}\alpha_1 e^2 A^2)U$.²⁵ Indeed, it approaches the result for the interaction-quench problem^{26,27} in the limit of $\Omega \rightarrow \infty$. The Higgs mode is amplified by the ac electric field around $2\Omega = 2\Delta$. The term decays algebraically as $t^{-1/2}$,² which suggests that the Higgs mode effectively has an infinite lifetime within the BCS approximation.

In the long-time limit, the constant term and the term oscillating with frequency 2Ω survive. The constant term in $\delta\Delta(t)$ is proportional to $\alpha_1(1 - \lambda^{-1})$, which implies, intriguingly, that we can attain an *amplification* of superconductivity on time average when this term is positive. The 2Ω oscillation term represents the APR. If we write the last term in Eq. (23) as $\frac{1}{4\lambda}\mathcal{A}\cos(2\Omega t - \varphi)$, the amplitude \mathcal{A} and the phase shift φ are universal functions that depend only on the ratio $2\Omega/2\Delta$ (Fig. 4). The amplitude \mathcal{A} diverges as $|2\Omega - 2\Delta|^{-1/2}$ at $2\Omega = 2\Delta$ (resonance condition). It clearly differs from the result of the time-dependent GL (8), $|2\Omega - 2\Delta|^{-1}$. The reduction of the power from 1 to 1/2 signifies that the Higgs mode is a bit less stable, where each pseudospin precession gradually dephases. Physically we can interpret this as coming from Landau damping; that is, the collective mode decays into individual quasiparticle excitations even in the collisionless equation (15). An anomaly is also found in the phase shift φ : for $2\Omega < 2\Delta$, φ is locked to zero, i.e., the 2Ω oscillation of the order parameter is in-phase with $E(t)^2$. As soon as 2Ω exceeds 2Δ , the φ discontinuously jumps to $\pi/2$ and starts to drift (Fig. 4). Along with the order-parameter oscillation, the pseudospin itself continues to precess around the axis parallel to $\sigma_k(0)$, with two modes of frequencies ω_k and 2Ω surviving in $t \rightarrow \infty$ (the former of which dephases). By numerically simulating Eq. (15), we also confirmed that APR generally occurs for finite-temperature initial states and for pulsed electric fields that contain large enough number of oscillation cycles.

APR appears in various physical quantities. What is readily accessible experimentally is the electric current,

$$\mathbf{j} = e \sum_{k,\sigma} \mathbf{v}_{k-eA(t)} c_{k\sigma}^\dagger c_{k\sigma} \quad (25)$$

($\mathbf{v}_k = \nabla_k \epsilon_k$ is the group velocity). The current is expressed in the pseudospin notation as $\mathbf{j} = e \sum_k [\mathbf{v}_{k-eA(t)} - \mathbf{v}_{k+eA(t)}] \sigma_k^z + \frac{e}{2} \sum_{k\sigma} [\mathbf{v}_{k-eA(t)} + \mathbf{v}_{k+eA(t)}] c_{k\sigma}^\dagger c_{k\sigma}$. If we expand it in $A(t)$, the linear response is given by $\mathbf{j}^{(1)} = -2\alpha_1 e^2 A(t) \sum_k \epsilon_k \sigma_k^z(0) + e \sum_{k\sigma} \mathbf{v}_k c_{k\sigma}^\dagger c_{k\sigma}$, which is irrelevant to APR. In fact, the linear-response optical conductivity does not show any divergence for $\Omega \neq 0$.²⁸ The leading term that reflects the change of the order parameter is the third-harmonic generation (THG),

$$\mathbf{j}^{(3)}(t) = -2\alpha_1 e^2 \Delta U^{-1} \delta\Delta(t) A(t), \quad (26)$$

where we have used $\epsilon_k \delta\sigma_k^z = \Delta \delta\sigma_k^x$. The consequence is remarkable: although the frequency Ω is below the energy gap, we do obtain the colossal nonlinear response due to divergence of $\delta\Delta(t)$. It may be used as an efficient THz harmonic emitter.

IV. RESPONSE FUNCTION FOR ANDERSON PSEUDOSPIN RESONANCE

To reinforce our picture for APR phenomenon, we can approach it from an alternative, diagrammatic point of view. This allows one to decompose the THG susceptibility into the bare and vertex-correction diagrams, each of which contains individual and collective excitations, respectively. Thus we can unambiguously distinguish the Higgs mode from quasiparticle excitations that are degenerate at the superconducting gap energy. To this end, we take the Nambu-Gor'kov Green's function defined by

$$\hat{G}_k(t, t') = \begin{pmatrix} -i\langle \mathcal{T} c_{k\uparrow}(t) c_{k\uparrow}^\dagger(t') \rangle & -i\langle \mathcal{T} c_{k\uparrow}(t) c_{-k\downarrow}(t') \rangle \\ -i\langle \mathcal{T} c_{-k\downarrow}^\dagger(t) c_{k\uparrow}^\dagger(t') \rangle & -i\langle \mathcal{T} c_{-k\downarrow}^\dagger(t) c_{-k\downarrow}(t') \rangle \end{pmatrix},$$

where \mathcal{T} represents the time ordering. With this, the gap function is expressed as

$$\Delta(t) = -\frac{i}{2} U \sum_k \text{Tr} [\tau_1 \hat{G}_k^<(t, t)], \quad (27)$$

where $\hat{G}_k^<$ is the lesser Green's function, and $\Delta(t)$ is assumed to be real.

Now we take variations of both sides of Eq. (27) with respect to the external field $A(t)$. In this section, we consider the monochromatic wave $A(t) = A e^{-i\Omega t}$. Since the leading change of the order parameter $\delta\Delta(t) = \delta\Delta e^{-2i\Omega t}$ is the second order in $A(t)$, we have

$$\delta\Delta = \delta_A^2 \Delta = -\frac{i}{2} U \sum_k \text{Tr} [\tau_1 \delta_A^2 \hat{G}_k^<], \quad (28)$$

where δ_A represents the functional derivative with respect to A . In the BCS theory, the Nambu-Gor'kov Green's function is given by the Dyson equation $\hat{G}_k = (i\partial_t - \hat{\xi}_k + \Delta\tau_1)^{-1}$ with $\hat{\xi}_k \equiv \xi_k - eA\tau_3$. Hence the variation of the order parameter reads

$$\begin{aligned} \delta_A^2 \Delta &= -iU \sum_k \text{Tr} [\tau_1 \hat{G}_k (\delta_A \hat{\xi}_k) \hat{G}_k (\delta_A \hat{\xi}_k) \hat{G}_k^<] \\ &\quad - \frac{i}{2} U \sum_k \text{Tr} [\tau_1 \hat{G}_k (\delta_A^2 \hat{\xi}_k - \delta_A^2 \Delta \tau_1) \hat{G}_k^<]. \end{aligned} \quad (29)$$

Here the lesser component of the products of the Green's functions should be understood by Langreth's rule [e.g., $(GG)^< = G^R G^< + G^< G^A$]. Equation (29) determines $\delta\Delta = \delta_A^2 \Delta$ self-consistently. This is diagrammatically represented in the first line of Fig. 5. One can show that the first term on the right hand side of Eq. (29) vanishes in the BCS theory. By solving Eq. (29) in the frequency domain, we end up with

$$\delta\Delta = \frac{\frac{i}{2}\alpha_1 U \sum_{k,\omega} \xi_k \text{Tr} [\tau_1 \hat{G}_k(\omega + 2\Omega) \tau_3 \hat{G}_k(\omega)]^<}{1 - \frac{i}{2} U \sum_{k,\omega} \text{Tr} [\tau_1 \hat{G}_k(\omega + 2\Omega) \tau_1 \hat{G}_k(\omega)]^<}. \quad (30)$$

Note that $\langle \tau_1 \hat{G}_k \tau_1 \hat{G}_k \rangle$ appearing in the denominator is the dynamical pair-pair correlation function.

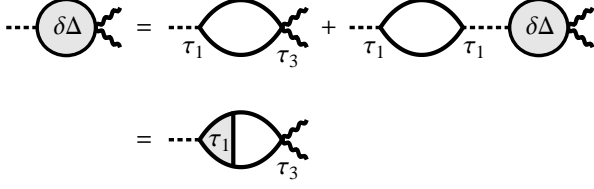


FIG. 5: The diagrammatic representation of the self-consistent Eq. (29) for $\delta\Delta$ and its relation to the τ_1 vertex. The wavy and dashed lines represent the gauge field A and the interaction vertices, respectively.

The amplitude of the 2Ω oscillation of $\delta\Delta$ diverges (i.e., APR occurs) when the denominator of Eq. (30) vanishes due to fluctuations in the τ_1 channel. Thus the resonance sensitively reflects the structure of the pair-pair correlation function. We should emphasize that the τ_1 fluctuation appears without considering self-energy corrections beyond the mean-field BCS formalism. Namely, the τ_1 fluctuation is already present in the response to electromagnetic fields in the BCS regime before we further include fluctuations by, e.g., the random phase approximation.

As indicated in the second line of Fig. 5, $\delta\Delta$ can also be expressed in terms of the τ_1 vertex. Formally, the Higgs mode is defined as a pole of the τ_1 vertex. Therefore, the divergence of $\delta\Delta$ can indeed be rephrased as a resonance with the Higgs mode.

The explicit calculation for the correlation functions within the BCS theory enables one to write down $\delta\Delta$ (30) analytically as

$$\delta\Delta = \frac{1}{2}\alpha_1 e^2 A^2 \Delta \left[\frac{1}{\lambda R(\Omega, T)} - 1 \right], \quad (31)$$

where the resonance function $R(\Omega, T)$ is given by

$$R(\Omega, T) = \mathcal{P} \int_{\Delta}^{\infty} d\omega \frac{\Omega^2 - \Delta^2}{(\Omega^2 - \omega^2) \sqrt{\omega^2 - \Delta^2}} \tanh\left(\frac{\omega}{2T}\right) - \frac{i\pi}{2} \theta(\Omega - \Delta) \frac{\sqrt{\Omega^2 - \Delta^2}}{\Omega} \tanh\left(\frac{\Omega}{2T}\right) \quad (32)$$

with \mathcal{P} denoting the principal value of the integral.

In the limit of $2\Omega \rightarrow 2\Delta$ (i.e., $\Omega \rightarrow \Delta$), $R(\Omega, T)$ has an asymptotic form of

$$R(\Omega, T) \sim \begin{cases} \frac{\pi}{2} \frac{\sqrt{\Delta^2 - \Omega^2}}{\Delta} \tanh\left(\frac{\Delta}{2T}\right) & \Omega \rightarrow \Delta - 0 \\ -\frac{i\pi}{2} \frac{\sqrt{\Omega^2 - \Delta^2}}{\Delta} \tanh\left(\frac{\Delta}{2T}\right) & \Omega \rightarrow \Delta + 0. \end{cases} \quad (33)$$

Hence $|\delta\Delta|$ diverges in this limit as

$$|\delta\Delta| \sim \frac{\alpha_1 e^2 A^2 \Delta^2}{\pi \lambda \tanh\left(\frac{\Delta}{2T}\right)} \frac{1}{|\Omega^2 - \Delta^2|^{1/2}}. \quad (34)$$

Remarkably, the divergence persists at arbitrary temperatures $T < T_c$ with the fixed critical exponent $\frac{1}{2}$, which indicates that the APR is robust against thermal fluctuations.

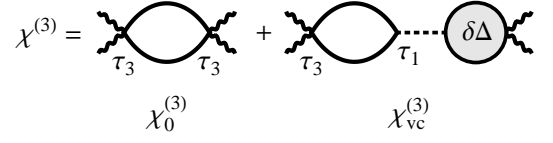


FIG. 6: Feynman diagram for the THG susceptibility of superconductors. The first and second terms on the right-hand side correspond to $\chi_0^{(3)}$ and $\chi_{vc}^{(3)}$, respectively.

In the zero-temperature limit, $R(\Omega, T)$ is reduced to

$$R(\Omega, T) \xrightarrow{T \rightarrow 0} \begin{cases} \frac{\sqrt{\Delta^2 - \Omega^2}}{\Omega} \sin^{-1}\left(\frac{\Omega}{\Delta}\right) & \Omega < \Delta \\ \frac{\sqrt{\Omega^2 - \Delta^2}}{\Omega} \left[\cosh^{-1}\left(\frac{\Omega}{\Delta}\right) - i\frac{\pi}{2} \right] & \Omega > \Delta. \end{cases} \quad (35)$$

Plugging this into Eq. (31), one can see that it precisely reproduces the result (23) derived in the previous section [note that the seeming difference of the factor $\frac{1}{2}$ is due to the assumption of $A(t) = A e^{-i\Omega t}$ in the present section and $A(t) = A \sin \Omega t$ in the previous section].

In the language of the Green's function, the current is given by

$$j(t) = ie \sum_k \text{Tr} [\hat{v}_k \hat{G}_k^<(t, t)], \quad (36)$$

where $\hat{v}_k \equiv v_{k-eA(t)\tau_3}$. If we focus on the THG response that is relevant to APR, we can take the third derivative with respect to $A(t)$ to obtain

$$j^{(3)} = ie \sum_k \text{Tr} [(\delta_A^3 \hat{v}_k) \hat{G}_k^<] + ie \sum_k \text{Tr} [(\delta_A \hat{v}_k) \hat{G}_k (\delta_A^2 \hat{\xi}_k - \delta_A^2 \Delta \tau_1) \hat{G}_k]. \quad (37)$$

Here we have used the fact that odd-order derivatives of $\hat{G}_k^<(t, t)$ vanish as indicated by the pseudospin analysis [see Eqs. (16)-(18)].

The first term in Eq. (37) is of higher order in (ω_D/ϵ_F) than the other terms, so that it is negligible. Then the leading contributions to $j^{(3)}$ are the second and third terms, which we write as

$$j^{(3)} = \chi_{\text{tot}}^{(3)} A^3 = (\chi_0^{(3)} + \chi_{vc}^{(3)}) A^3. \quad (38)$$

$\chi_{\text{tot}}^{(3)}$ is the total THG susceptibility, which comprises the bare susceptibility $\chi_0^{(3)}$ and vertex correction $\chi_{vc}^{(3)}$. The Feynman diagram for these is depicted in Fig. 6. Here one can single out the contribution of the 2Ω collective oscillation of the order parameter to the THG signal, which is $\chi_{vc}^{(3)}$. In other words, we can distinguish the effect of quasiparticle excitations from the contribution of the Higgs mode.

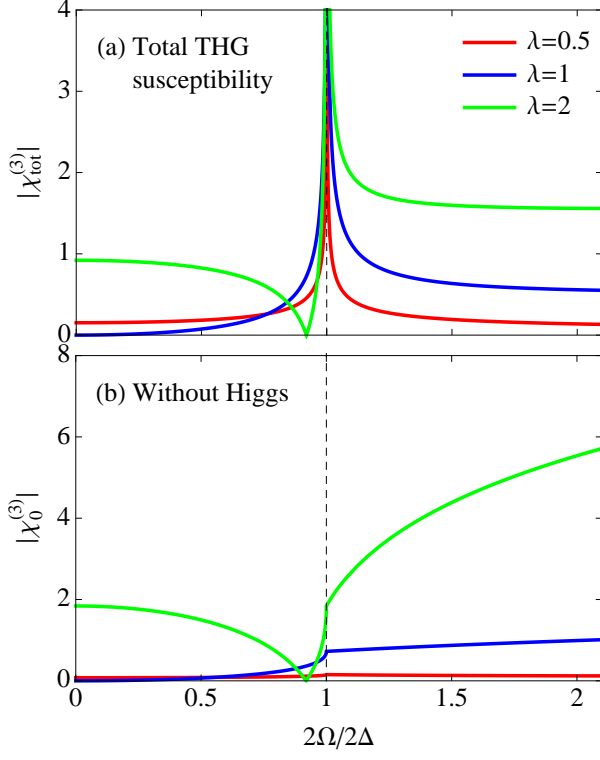


FIG. 7: (Color online) The amplitude of (a) the full and (b) bare THG susceptibilities for superconductors at $T = 0$ with $\lambda = 0.5, 1, 2$ in units of $a_1^2 e^4 \omega_D^2 D(\epsilon_F)$.

We can evaluate the components of the susceptibility explicitly in the BCS theory with the function $R(\Omega, T)$ (32) as

$$\chi_0^{(3)} = a_1^2 e^4 \frac{\Delta^2}{U} [\lambda R(\Omega, T) - 1], \quad (39)$$

$$\chi_{vc}^{(3)} = -a_1^2 e^4 \frac{\Delta^2}{U} \frac{[\lambda R(\Omega, T) - 1]^2}{\lambda R(\Omega, T)}. \quad (40)$$

Taking the sum of the two susceptibilities, we obtain the total contribution,

$$\chi_{\text{tot}}^{(3)} = \chi_0^{(3)} + \chi_{vc}^{(3)} = -a_1^2 e^4 \frac{\Delta^2}{U} \left[\frac{1}{\lambda R(\Omega, T)} - 1 \right]. \quad (41)$$

With Eqs. (31) and (41), we reproduce the previous relation (26). Note that the term $\lambda R(\Omega, T)$ appears in the denominator for $\chi_{\text{tot}}^{(3)}$ and in the numerator for $\chi_0^{(3)}$ in the opposite ways.

In Fig. 7, we plot $\chi_{\text{tot}}^{(3)}$ along with $\chi_0^{(3)}$ for several values of λ at $T = 0$. When we change λ , we evaluate the gap by $\Delta = \omega_D / \sinh(1/\lambda)$. We can see that $\chi_{\text{tot}}^{(3)}$ diverges in a similar manner as $\delta\Delta$ (Fig. 4) at $2\Omega = 2\Delta$, while $\chi_0^{(3)}$ only shows kink structures. This endorses that the resonance peak is indeed a manifestation of the effect of the Higgs mode, and cannot be explained by quasiparticle excitations or pair breaking contained in $\chi_0^{(3)}$. As one increases λ , the amplitude of the divergence becomes larger. For $\lambda > 1$, $\chi_{\text{tot}}^{(3)}$ and $\chi_0^{(3)}$ vanish at the value of $2\Omega/2\Delta$ at which $\lambda R(\Omega, T) = 1$ is satisfied. Consequently, the susceptibility spectrum shows a sharp dip structure. This can be exploited to experimentally discern whether

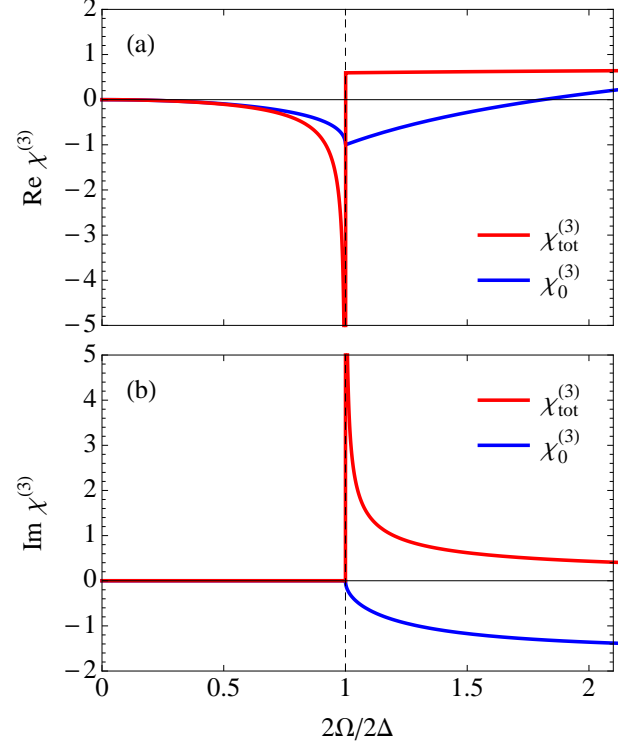


FIG. 8: (Color online) (a) The real and (b) imaginary parts of the THG susceptibility for superconductors at $T = 0$ with $\lambda = 1$ in units of $a_1^2 e^4 \omega_D^2 D(\epsilon_F)$.

$\lambda > 1$ or not. We also notice that the shape of the resonance peak is significantly asymmetric about $2\Omega = 2\Delta$, which becomes more prominent for larger λ . The asymmetry originates from the mixing of the collective mode (discrete level) with quasiparticle excitations (continuous levels). While this is reminiscent of the Fano resonance, the form of the resonance function is not identical with the Fano form.

If we look at the real and imaginary parts of the THG susceptibility in Fig. 8, the spectral features are again very different between $\chi_{\text{tot}}^{(3)}$ and $\chi_0^{(3)}$. $\text{Re} \chi_{\text{tot}}^{(3)}$ and $\text{Im} \chi_{\text{tot}}^{(3)}$ diverge as $\Omega \rightarrow \Delta - 0$ and $\Omega \rightarrow \Delta + 0$, respectively, whereas $\text{Re} \chi_0^{(3)}$ remains finite and $\text{Im} \chi_0^{(3)}$ vanishes in these limits. Both $\chi_{\text{tot}}^{(3)}$ and $\chi_0^{(3)}$ have zero imaginary parts at $\Omega < \Delta$. This simply reflects that photo-absorption is not allowed with frequencies below the energy gap even in the nonlinear-response regime.

If we turn to the temperature dependence of the THG susceptibility in Fig. 9, $\chi_{\text{tot}}^{(3)}$ diverges for temperatures $T < T_c$, similarly to the behavior of $\delta\Delta$ (34). The shape of the resonance peak does not change significantly against temperature. The insensitivity of the THG signal against temperature should facilitate experiments where a scan of the pump frequency Ω is difficult: one can instead scan temperature to change Δ for a fixed Ω . In Ref. 14, the THG resonance peak was in fact mapped out in this way.

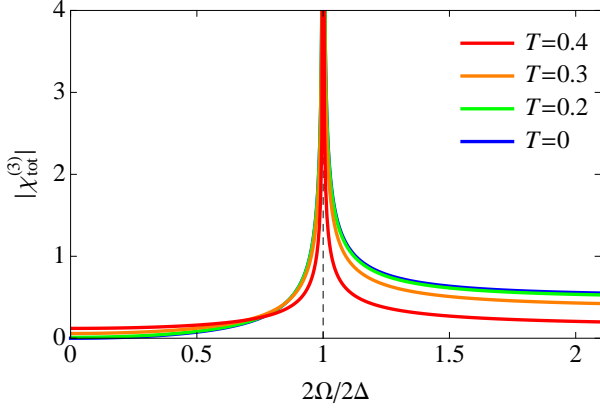


FIG. 9: (Color online) The temperature dependence of the THG susceptibility for superconductors with $\lambda = 1$ in units of $\alpha_1^4 e^4 \omega_D^2 D(\epsilon_F)$. Here, $T_c = 0.446$.

V. EFFECT OF ELECTRON-ELECTRON SCATTERING

So far, the argument has been based on the pairing Hamiltonian (9), which has the long-range interaction in real space. For more realistic models of superconductivity with short-range interactions, the analysis above is considered to be a static mean-field approximation, whose validity is restricted to the weak-coupling regime. Furthermore, the equation of motion (15) does not involve thermalization processes, which correspond to changes in the pseudospin length $|\sigma_k|$ due to correlation effects. Thus let us go beyond the static mean field by considering the attractive Hubbard model with a driving ac field,

$$H_{\text{Hubbard}} = \sum_{k\sigma} \epsilon_k - eA(t) c_{k\sigma}^\dagger c_{k\sigma} - U \sum_i c_{i\uparrow}^\dagger c_{i\uparrow} c_{i\downarrow}^\dagger c_{i\downarrow}, \quad (42)$$

where i labels the lattice sites and U is an attractive Hubbard interaction. We take, as an example, a one-dimensional dispersion $\epsilon_k = -2 \cos k$ with the bandwidth $W = 4$ and $\alpha_1 = -1$ (later in this section we also consider an infinite-dimensional lattice). We calculate the time evolution by means of the nonequilibrium dynamical mean-field theory (DMFT)^{29–31}, which is extended here to the Nambu formalism for treating superconductors. For an impurity solver for DMFT, we employ the third-order perturbation theory³², which is supposed to be reliable in the region $U < W$. The system is set at half filling with $U = 3.5$, which belongs to a strong-coupling regime ($2\Delta_{T=0}/T_c \approx 5.0$ well above the BCS value).

The time evolution of the local superconducting order parameter, $\Phi(t) = \langle c_{i\uparrow}^\dagger c_{i\downarrow}^\dagger \rangle$, for various initial temperatures (β^{-1}) is shown in Fig. 10. With increased total energy due to the continuous excitation, the overall value of the order parameter gradually decreases. On top of that, the coherent oscillation of the order parameter with frequency 2Ω emerges [with the same oscillation period of $E(t)^2$ shown in Fig. 10]. The oscillation is particularly enhanced around $\beta = 6.5$, and becomes invisible for $\beta = 9.0$. The phase-shift anomaly is not clearly observed in this interaction regime. We evaluate the

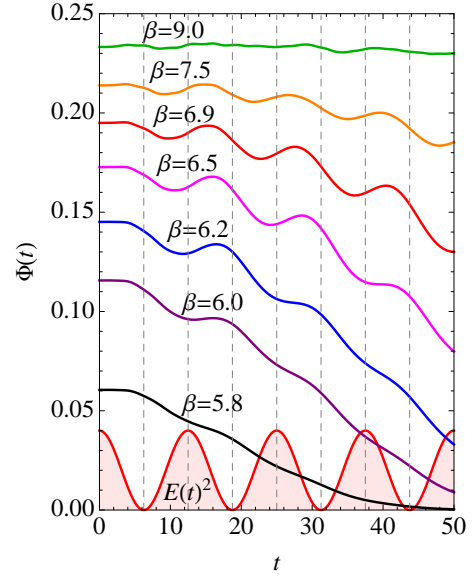


FIG. 10: (Color online) Temporal evolution of the superconducting order parameter $\Phi(t)$ calculated with the nonequilibrium DMFT for the attractive Hubbard model with the 1D density of states at half filling driven by an ac field with $U = 3.5$, $A = 0.15$, and $\Omega = 2\pi/25$ for several temperatures (β^{-1}) for the initial states. The sinusoidal curve represents $E(t)^2 \propto \cos^2 \Omega t$. Dashed lines are a guide to the eye.

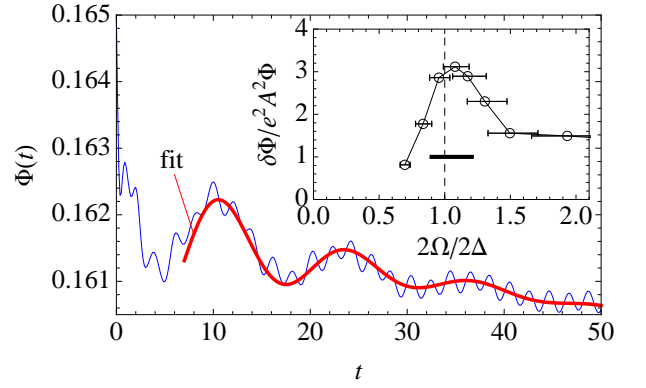


FIG. 11: (Color online) Temporal evolution of the order parameter $\Phi(t)$ after a quench $U \rightarrow U - \delta U$ at $t = 0$ with $U = 3.5$ and $\delta U = 0.01$ in the attractive Hubbard model at $\beta = 6.4$. The rapid oscillation comes from a band-edge effect, while the slower one corresponds to the Higgs mode. Thick (red) curve is a fit (see text). Inset: The amplitude of the 2Ω oscillating component of the order parameter $\delta\Phi$ for the attractive Hubbard model driven by an ac field with $U = 3.5$, $\Omega = 2\pi/25$, and various Δ . The bar shows the width estimated from the lifetime of the Higgs mode.

energy gap 2Δ in equilibrium from the single-particle spectral function $A(\omega)$, which is calculated by Fourier transformation of the real-time simulation. If we measure the amplitude of the 2Ω oscillation of the order parameter, $\delta\Phi$, at the third cycle, we can clearly see in the inset of Fig. 11 that a resonance peak indeed emerges at $2\Omega = 2\Delta$ (the error bars represent inaccuracy in measuring Δ). The peak position corresponds to

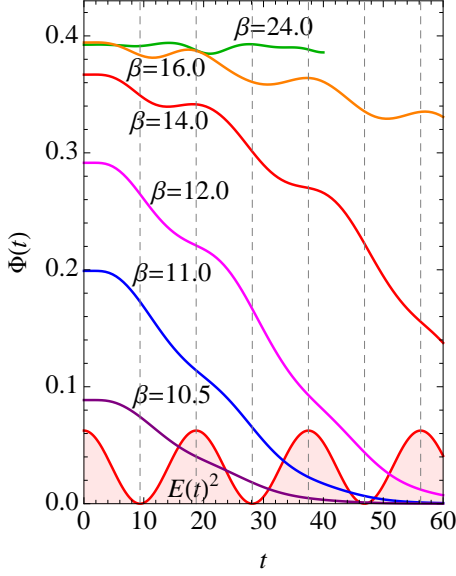


FIG. 12: (Color online) Temporal evolution of the superconducting order parameter $\Phi(t)$ calculated with the nonequilibrium DMFT for the attractive Hubbard model with the infinite-dimensional (Gaussian) density of states at half filling driven by the ac field with $U = 2.25$, $A = 0.2$, and $\Omega = 2\pi/37.5$, for several temperatures (β^{-1}) for the initial states. The sinusoidal curve represents $E(t)^2 \propto \cos^2 \Omega t$. Dashed lines are a guide to the eye.

$\beta \approx 6.4$. The result indicates that APR indeed exists beyond the static mean-field level.

However, we do notice a deviation from the BCS result; i.e., the resonance has a finite width (the inset of Fig. 11). There are several factors that determine the resonance width. Besides extrinsic experimental factors such as the limited measurement time scale or energy dissipation to external environment (which is absent in our calculations), one intrinsic factor is the finite lifetime τ of the Higgs amplitude mode, which can decay into individual excitations [note that Higgs does not decay into the Nambu-Goldstone (NG) mode in charged superconductors, since the energy of the NG mode is lifted to the plasma frequency, at least away from the critical regime near $T = T_c$]. If the Higgs mode decays exponentially, the poles $s = \pm 2i\Delta$ acquire a real part on the complex plane (Fig. 3), and are thus prevented from meeting the branching points $\pm 2i\Omega$, resulting in broadening of the resonance peak. We can numerically evaluate the decay rate by generating the Higgs mode at $\beta = 6.4$ with a small perturbation (here we use an interaction quench³³), where $\Phi(t)$ is fitted with $\Phi_0 e^{-t/\tau} \cos(2\Delta t + \theta)$ on top of a linear drift (Fig. 11). A rapid oscillation in Fig. 11 comes from the divergence of the 1D density of states at band edges, and is irrelevant to the Higgs mode. From the derived τ , we estimate the resonance width as indicated by the bar in the inset of Fig. 11, which roughly coincides with the peak width of APR with the background subtracted (Fig. 11).

While we have applied the nonequilibrium DMFT to a system with 1D density of states for simplicity, we can actu-

ally confirm that the result does not change qualitatively for the infinite-dimensional hypercubic lattice with the Gaussian density of states $D(\epsilon) = e^{-\epsilon^2}/\sqrt{\pi}$, where the DMFT formalism is no longer an approximation but becomes exact. Let us consider the hypercubic lattice with the electric field applied along the diagonal direction, $A(t) = A(t)(1, 1, 1, \dots)$. The energy dispersion reads^{30,34}

$$\epsilon_{k-A(t)} = \epsilon_k \cos A(t) + \bar{\epsilon}_k \sin A(t), \quad (43)$$

where $\epsilon_k = -1/\sqrt{d} \sum_{i=1}^d \cos k_i$ and $\bar{\epsilon}_k = -1/\sqrt{d} \sum_{i=1}^d \sin k_i$. This makes the momentum summation of the lattice Green's function in the nonequilibrium DMFT a double integral with respect to ϵ and $\bar{\epsilon}$. The double integral becomes computationally very heavy, especially in the present case where we have to keep track of the system evolving over a long enough interval to capture the slow order-parameter dynamics. To overcome the difficulty here we make use of the following formula,

$$\begin{aligned} & \sum_k G_k(t, t') \\ &= \int d\epsilon d\bar{\epsilon} D(\epsilon) D(\bar{\epsilon}) (i\partial_t + \mu - \epsilon \cos A - \bar{\epsilon} \sin A - \Sigma)^{-1} \\ &= \frac{1}{2} \left[\int d\epsilon D(\epsilon) \left(i\partial_t + \mu - \epsilon \cos A - \frac{1}{\sqrt{2}} \sin A - \Sigma \right)^{-1} \right. \\ & \quad \left. + \int d\bar{\epsilon} D(\bar{\epsilon}) \left(i\partial_t + \mu - \epsilon \cos A + \frac{1}{\sqrt{2}} \sin A - \Sigma \right)^{-1} \right] \\ & \quad + O(A^3), \end{aligned} \quad (44)$$

to reduce the double integral to a single one, where μ is the chemical potential, Σ is the self-energy, and we have used $\int d\bar{\epsilon} D(\bar{\epsilon}) \bar{\epsilon}^2 = 1/2$. The formula is valid up to the second order in A , which is sufficient for the present purpose, since our interest is in the order-parameter oscillation arising from the second-order nonlinear effect. An advantage of the above formula is that the first and second terms are in the form of the Green's function with $\bar{\epsilon}$ replaced by $\pm 1/\sqrt{2}$, so that the implementation is straightforward. We also remark that keeping the form of the Green's function is vital for maintaining the numerical stability. As an impurity solver for the nonequilibrium DMFT for the hypercubic lattice, here we employ the second-order iterative perturbation theory³² to further reduce the computational cost. If we look at the time evolution of the order parameter in the infinite-dimensional hypercubic lattice in Fig. 12, the 2Ω oscillation of the order parameter is prominent around $\beta = 14.0$ and 16.0 , which is close to the resonance condition $2\Omega (= 4\pi/37.5 = 0.335) = 2\Delta (\approx 0.32, \text{ evaluated from the nonequilibrium DMFT calculation for the spectral function})$. Away from this, the oscillation tends to be suppressed and the oscillation becomes incoherent. This shows that APR also occurs in the nonequilibrium DMFT calculation for the infinite-dimensional lattice where DMFT becomes exact. Thus the essential features of APR do not depend on a particular form of the density of states.

VI. SUMMARY

To summarize, we theoretically propose a phenomenon that may be called Anderson pseudospin resonance (APR) for a superconductor driven by an ac electric field, which is confirmed by solving the equation of motion analytically within the BCS approximation, and by solving the attractive Hubbard model via the nonequilibrium DMFT. APR can be distinguished from quasiparticle excitations or pair breaking processes near the superconducting gap energy by looking at the divergent enhancement of third harmonic generation. APR provides not only a new pathway of controlling superconductors, but also

provides an avenue offering information about dynamical aspects of the order parameter and the Higgs mode in superconductors. Important future problems include whether APR occurs for other pairing symmetries such as the anisotropic d -wave pairing.

We wish to thank R. Shimano, R. Matsunaga, H. Fujita, and A. Sugioka for stimulating discussions that motivate the present project and providing their experimental data. We were supported by a Grant-in-Aid for Scientific Research from MEXT (No. 26247057), and N.T. by Grant-in-Aid for Scientific Research from JSPS (No. 25104709 and No. 25800192).

-
- ¹ P. W. Anderson, Phys. Rev. **112**, 1900 (1958).
 - ² A. F. Volkov and S. M. Kogan, Sov. Phys. JETP **38**, 1018 (1974).
 - ³ P. B. Littlewood and C. M. Varma, Phys. Rev. Lett. **47**, 811 (1981); Phys. Rev. B **26**, 4883 (1982).
 - ⁴ C. Varma, J. Low Temp. Phys. **126**, 901 (2002).
 - ⁵ D. Pekker and C. Varma, Annual Review of Condensed Matter Physics **6**, 269 (2015).
 - ⁶ F. Englert and R. Brout, Phys. Rev. Lett. **13** 321, (1964).
 - ⁷ P. W. Higgs, Phys. Lett. **12**, 132 (1964); Phys. Rev. Lett. **13**, 508 (1964).
 - ⁸ G. S. Guralnik, C. R. Hagen, and T. W. B. Kibble, Phys. Rev. Lett. **13**, 585 (1964).
 - ⁹ Y. Nambu and G. Jona-Lasinio, Phys. Rev. **122**, 345 (1961).
 - ¹⁰ P. W. Anderson, Phys. Rev. **130**, 439 (1963).
 - ¹¹ R. Sooryakumar and M. V. Klein, Phys. Rev. Lett. **45**, 660 (1980).
 - ¹² M.-A. Méasson, Y. Gallais, M. Cazayous, B. Clair, P. Rodière, L. Cario, and A. Sacuto, Phys. Rev. B **89**, 060503 (2014).
 - ¹³ R. Matsunaga, Y. I. Hamada, K. Makise, Y. Uzawa, H. Terai, Z. Wang, and R. Shimano, Phys. Rev. Lett. **111**, 057002 (2013).
 - ¹⁴ R. Matsunaga, N. Tsuji, H. Fujita, A. Sugioka, K. Makise, Y. Uzawa, H. Terai, Z. Wang, H. Aoki, and R. Shimano, Science **345**, 1145 (2014).
 - ¹⁵ ATLAS Collaboration, Phys. Lett. B **716**, 1 (2012).
 - ¹⁶ CMS Collaboration, Phys. Lett. B **716**, 30 (2012).
 - ¹⁷ L. P. Gor'kov, Sov. Phys. JETP **9**, 1364 (1959).
 - ¹⁸ N. N. Bogoliubov, V. V. Tolmachev, and D. V. Shirkov, *A New Method in the Theory of Superconductivity* (Achademy of Sciences of USSR, Moscow, 1958).
 - ¹⁹ Y. Nambu, Physica **15D**, 147 (1985).
 - ²⁰ G. E. Volovik and M. A. Zubkov, Phys. Rev. D **87**, 075016 (2013); J. Low Temp. Phys. **175**, 486 (2014).
 - ²¹ R. A. Barankov, L. S. Levitov, and B. Z. Spivak, Phys. Rev. Lett. **93**, 160401 (2004).
 - ²² E. A. Yuzbashyan, B. L. Altshuler, V. B. Kuznetsov, and V. Z. Enolskii, Phys. Rev. B **72**, 220503 (2005).
 - ²³ B. Mansart, J. Lorenzana, A. Mann, A. Odeh, M. Scarongella, M. Chergui, and F. Carbone, Proc. Natl. Acad. Sci. **110**, 4539 (2013).
 - ²⁴ J. Lorenzana, B. Mansart, A. Mann, A. Odeh, M. Chergui, and F. Carbone, Eur. Phys. J. Special Topics **222**, 1223 (2013).
 - ²⁵ N. Tsuji, T. Oka, and H. Aoki, Phys. Rev. Lett. **103**, 047403 (2009).
 - ²⁶ R. A. Barankov and L. S. Levitov, Phys. Rev. Lett. **96**, 230403 (2006).
 - ²⁷ E. A. Yuzbashyan and M. Dzero, Phys. Rev. Lett. **96**, 230404 (2006).
 - ²⁸ W. Zimmermann, E. Brandt, M. Bauer, E. Seider, and L. Genzel, Physica C: Supercond. **183**, 99 (1991).
 - ²⁹ J. K. Freericks, V. M. Turkowski, and V. Zlatić, Phys. Rev. Lett. **97**, 266408 (2006).
 - ³⁰ H. Aoki, N. Tsuji, M. Eckstein, M. Kollar, T. Oka, and P. Werner, Rev. Mod. Phys. **86**, 779 (2014).
 - ³¹ Note that what essentially matters in the DMFT calculation here is the density of states near the Fermi energy and the α_1 parameter. Thus, one may take our model adopted here as a certain infinite-dimensional lattice model that has the corresponding density of states and α_1 , to which DMFT can be applied.
 - ³² N. Tsuji and P. Werner, Phys. Rev. B **88**, 165115 (2013).
 - ³³ N. Tsuji, M. Eckstein, and P. Werner, Phys. Rev. Lett. **110**, 136404 (2013).
 - ³⁴ V. Turkowski and J. K. Freericks, Phys. Rev. B **71**, 085104 (2005).